

Tracy L. DeLiberty* and John A. Callahan
University of Delaware, Newark, Delaware

1 INTRODUCTION

The Amazon Basin plays an important role in the tropical climate and hydrology. It contains one of the major convective centers that fuels the general circulation of the atmosphere and its abundant rainfall feeds the largest freshwater stream of the world. The tropical forests provide habitats for about half of the world's species and are an important natural sink of CO_2 . Over the past decade, the Amazon Basin has received considerable attention from the scientific community as a result of the potential climatic and hydrologic impact of biomass burning and deforestation. Rates of deforestation in Brazilian Amazon have increased from 15,000 $km^2 yr^{-1}$ in the early 1990s to more than 18,000 $km^2 yr^{-1}$ in 1995 to 1998 (Laurance 2000).

Deforestation as a result of human activities is altering the conditions at the lower boundary of the atmosphere. Numerous modeling studies (e.g., Nobre et al. 1991, Costa and Foley 2000) have examined how the climate and hydrology of the basin may respond to deforestation. In order to evaluate possible anthropogenic impacts to the Amazon, we must improve our understanding of the "natural" climatic and hydrological processes operating within the basin. While long-term studies of the variability of precipitation (e.g., Paiva and Clarke 1995) and river discharge (e.g., Richey et al. 1989, Marengo 1995) have been examined, other components of the hydrologic cycle, such as evapotranspiration and atmospheric water vapor have not received the same level of attention.

Water vapor is an important link connecting various components of the hydrologic cycle and a better understanding of its role requires long-term observations of both small- and large-scale water vapor features. Recent studies of atmospheric moisture and its transport have focused on its seasonal cycle and interannual variability using atmospheric reanalysis data (e.g., Curtis and Hastenrath 1999, Zeng 1999) at larger temporal and spatial scales. Remote sensing from satellites provides the opportunity to monitor atmospheric water vapor at higher spatial and temporal resolution than conventional sources, such as surface and radiosonde networks or model analyses. Geostationary satellites, in particular, provide excellent temporal sampling to supply the needed observations to characterize the diurnal variability of PW. This paper presents a picture of the meso-scale moisture patterns and diurnal variations of satellite derived estimates in June and October of 1988.

2 SATELLITE RETRIEVAL ALGORITHM

The satellite retrieval algorithm used in this study is a physical split-window (PSW) technique initially developed by Jedlovec (1987) and first applied to GOES imagery by Guillory et al. (1993). The PSW technique exploits the differential absorption of water vapor in the 11 and 12 μm channels. In this procedure, an initial estimate of the state of the atmosphere must first be supplied. Using a radiative transfer model, the expected atmospheric radiative emission received at the satellite sensor in the 11 and 12 μm bands is calculated. From the perturbations between the expected and observed radiation, we can calculate an appropriate offset between the estimated and actual integrated water vapor content

* Corresponding author address: University of Delaware, Center for Climatic Research, Newark, DE 19716; email: tracyd@udel.edu.

and retrieve PW. A detailed discussion of the mathematical formulation of PSW can be found in Guillory (1991) and a thorough evaluation of the performance is given in Suggs et al. (1999).

3 DATA AND METHODOLOGY

Observed radiances were retrieved from the GOES Visible Infrared Spin Scan Radiometer (VISSR) Atmospheric Sounder (VAS) for 1988. The NCEP/NCAR Reanalysis Project data provided the first guess atmospheric fields applied as input to the PSW. These fields included 17 levels of air temperature and 6 levels of humidity at 6-hourly intervals.

The area under investigation is the Amazon River Basin as shown in Figure 1. The box surrounding the basin represents the extent of the GOES imagery and therefore the derived PW fields. Also shown in figure 1 are seven 5x5 degree "zones" identified to concentrate our analysis.

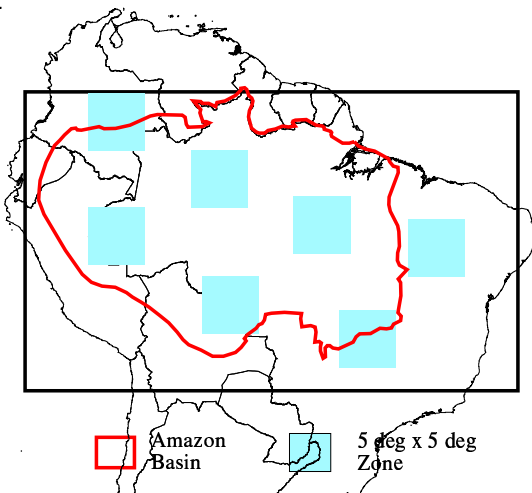


Figure 1: Study area encompasses the Amazon Basin and surrounding fringes. Box represents areal extent of geostationary imagery used in deriving PW with seven analysis zones outlined.

PW retrievals are made at a three-hourly time step during daylight hours for the months of June and October in 1988. Radiances are averaged using a 25 pixel neighborhood to minimize random noise in the sensor, thereby reducing the effective retrieval resolution to 40 km. Areas obscured by cloud cover are assigned the PW value of the first guess field from the Reanalysis data. Spatially continuous 0.5 degree fields are then generated 5 times daily at 12, 15, 18, 21 and 00Z, and then smoothed to reduce differences between PSW and the first guess values.

For each day, the maximum difference was computed among the 12Z, 15Z, 18Z, 21Z, and 00Z grids. A monthly average diurnal grid was then created and summarized by individual zones. The zones selected represent varying land surface and meteorological characteristics. When the PSW method is applied directly locations with radiosonde observations, PSW estimates PW reasonably well with MAE ranging from 3.0 to 9.0 mm and MAE/observed mean around 20%.

4 RESULTS

The geographic distribution of PW for June and October in 1988 is shown in Figure 2. A strong north-south gradient exists in June with a basin average of 38 mm. The highest PW values (over 55 mm) are found in the northwest, while the lowest (less than 25 mm) occur in the most southern and southeastern portions of the basin. In October the basin average is slightly higher at 41 mm, however, the spatial gradient is largely absent with higher PW throughout the area. More specifically, the monthly averages for zones 1 and 2 are between 45 and 50 mm, whereas zone 6 remains at 30 mm. The differences evident in June and October are largely due to changes in the large-scale circulation patterns and core centers of convection with the transition between the wet and dry seasons. In June, the ITCZ resides in the northern hemisphere causing surface winds to blow in an east-west direction into the mouth of the river. This draws in extremely moist air from the mid-Atlantic and allows periodic fronts to move up from the South Pacific High. In October, with the wet season just beginning, the ITCZ moves southward, pushing sur-

face winds in a more northeast-southwest direction. The subsidence of the South Pacific High and the increase of temperature produces a low pressure area over the basin, which increases precipitation and atmospheric water vapor.

The diurnal variations are among the most prominent modes of variability in the Amazon. The diurnal cycle exhibits marked regional variations, usually related to low-level, geographically tied circulations. The average diurnal range for June and October in 1988 is shown in Figure 3. Diurnal range of water vapor tends to increase as you move further south and east. June displays a north-south gradient of variation similar to the PW field, although with a negative correlation to PW. In October, many of the areas with large PW variations correspond to grasslands and non-forested areas (except for the southeast coast) and smaller variations correspond to areas with forested heavy precipitation areas, such as the northwest.

Figure 4 displays the daily diurnal range for three selected zones in both June and October. The y-axis represents the percent change from the daily mean (e.g., $100 \frac{PW_{range}}{PW_{mean}}$). Zone 1 shows little diurnal variation and remains fairly consistent throughout both months. Zones 4 and 6 show a much larger variation, nearly 40% in some instances. The spikes in the graph most likely represent synoptic events (cold surges) moving northward.

PW peaks earlier in the day during October than in June. For all zones, except zone 2, the peak time for PW was 1 to 2 time-steps (3 - 6 hours) earlier in October than in June. This may be accounted for by land surface changes between June and October. For example, October is at the end of the dry season when foliage cover is less than at the end of the wet season. Also, the months prior to October are peak burning seasons for deforestation activities, leaving the land surface void of thick vegetation than existed in June.

5 SUMMARY

This paper examines the geographic distribution and diurnal variability of satellite derived precipitable water for June and October in 1988 across the Ama-

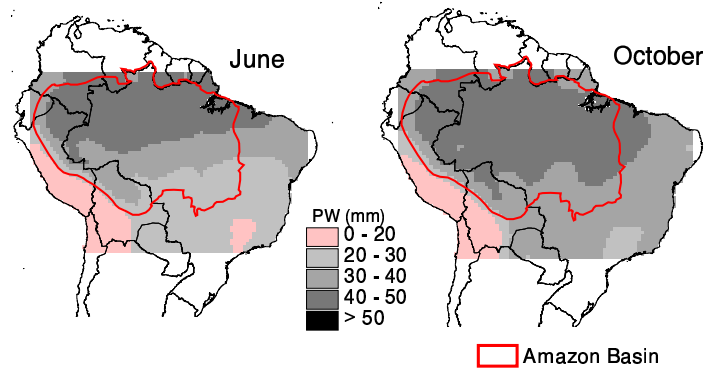


Figure 2: Average PSW-derived PW in 1988

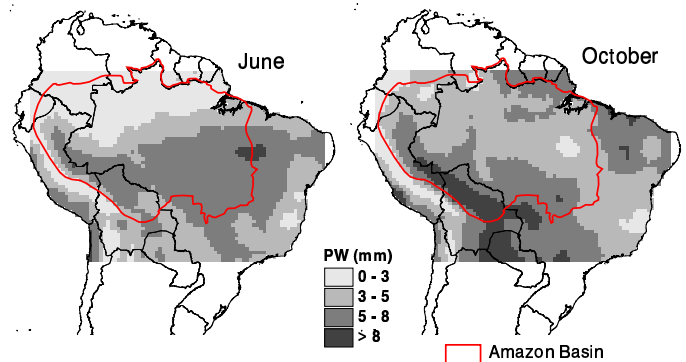


Figure 3: Average diurnal range of PSW-derived PW in 1988

zon Basin. The GOES estimates enables investigation of the moisture field at higher spatial and temporal scales than conventional radiosondes observations or model analyses. In addition, the PSW-derived estimates offers the opportunity to monitor the variability and trends over the region that may be evident as a result of biomass burning and deforestation.

6 ACKNOWLEDGMENTS

Special thanks is given to Dr. Paul Menzel and Ms. Elaine Prins in the early development of this

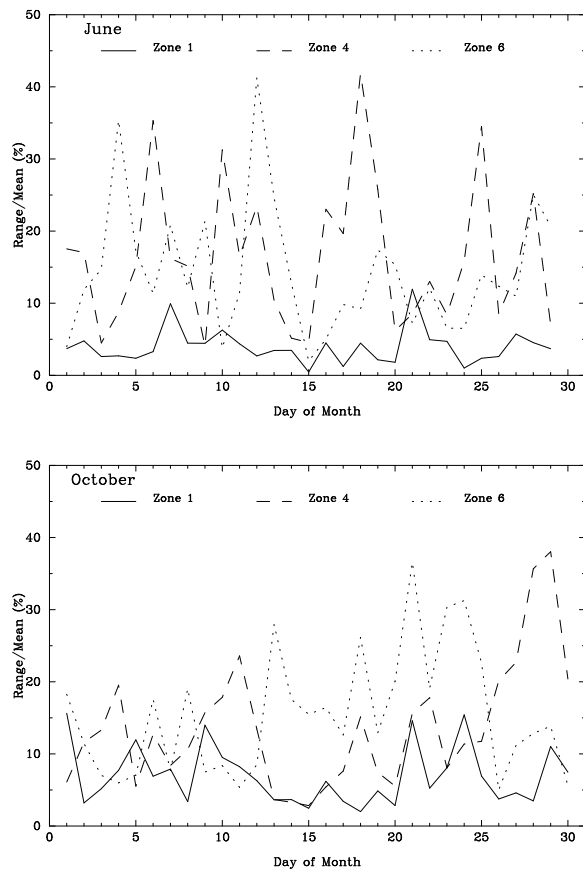


Figure 4: Diurnal range of PW in 1988 for Zone 1,4, and 6.

research and to Dr. Gary Jedlovec and Mr Anthony Guillory for assistance in using the PSW technique. Funding for this research was partially provided by the National Research Council's Associate-ships Program and the University of Delaware Research Foundation.

7 REFERENCES

Costa, M. H., and J. A. Foley, 2000: Combined effects of deforestation and doubled atmospheric CO_2 concentrations on the climate of Amazonia. *Journal of Climate*, 13(1), 18-34

Curtis, S. and S. Hastenrath, 1999: Trends of upper-air circulation and water vapor over equatorial South America and adjacent oceans. *International Journal of Climatology*, 19, 863-876.

Guillory, A. R., 1991: *A physical split window technique for deriving precipitable water utilizing VAS data*. M.S. Thesis, Florida State University, 70pp.

Guillory, A. R., G. J. Jedlovec, and H. E. Fuelberg, 1993: A technique for deriving column-integrated

water content using VAS split-window data. *Journal of Applied Meteorology*, 32, 1226-1241.

Jedlovec, G. J., 1987: *Determination of atmospheric moisture structure from high resolution MAMS radiance data*. Ph.D. Dissertation, University of Wisconsin-Madison, 187pp.

Laurance, W. F., 2000: Mega-development trends in the Amazon: Implications for global change. *Environmental Monitoring and Assessment*, 61(1), 113-122.

Marengo, J. A., 1995: Variations and change in South American streamflow. *Climatic Change*, 31, 99-117.

Nobre, C., P. J. Sellers, and J. Shukla, 1991: Amazonia deforestation and regional climate change. *Journal of Climate*, 4, 957-988.

Paiva, E. M. C. D., and R. T. Clarke, 1995: Time trends in rainfall records in Amazonia. *Bulletin of the American Meteorology Society*, 76(11), 2203-2209.

Richey, J. E., C. A. Nobre, and C. Deser, 1989: Amazon River discharge and climate variability: 1903-1985. *Science*, 246, 101-103.

Suggs, R. J., G. J. Jedlovec, and A. R. Guillory, 1998: Retrieval of geophysical parameters from GOES: Evaluation of a split window technique. *Journal of Applied Meteorology*, 37, 1205-1277.

Zeng, N., 1999: Seasonal cycle and interannual variability in the Amazon hydrologic cycle. *Journal of Geophysical Research*, 104(D8), 9097-9106.